Int. J. Math. And Appl., 6(3)(2018), 145–158
ISSN: 2347-1557
Available Online: http://ijmaa.in/

International Journal of *Mathematics And its Applications*

Transient Thermoelastic Analysis of a Multi-layered Oblate Spheroidal Shell with Internal Heat Generation

Tara Dhakate[1,*], Vinod Varghese[2] and Lalsingh Khalsa[1]

1 Department of Mathematics, Mahatma Gandhi Science College, Armori, Gadchiroli, India.

2 Department of Mathematics, Smt. Sushilabai Rajkamalji Bharti Science College, Arni, Yavatmal, India.

Abstract: The principal aim of this paper is to investigate the thermoelastic responses in a generalised oblate spheroid subjected time-independent volumetric heat sources in each layer and sectional heat supply on the inner and outer curved surfaces. The closed-form solution is obtained for transient temperature distributions by establishing Sturm-Liouville integral transform considering series expansion function in terms of an eigenfunction of Sturm-Liouville boundary value problem for the composite region consisting of multilayered composites in an oblate spheroidal coordinate system. The relations obtained in this paper can be applied to any arbitrary boundary and initial conditions to avoid structural failure due to thermal stress response. Some results which are derived using computational tools are accurate enough for the practical purpose were depicted graphically. The three-layer elliptic region has been computed numerically and exhibited in a graphical form, by using dimensionless values and therefore discussed.

MSC: 35B53, 35G30, 35K05, 44A10.

Keywords: multilayer oblate spheroid, transient heat conduction, thermal stresses, integral transform, composite.

 Accepted on: 21.05.2018

1. Introduction

An oblate spheroid is a surface generated by the rotation of an ellipse about its minor axis, and depending upon the ellipses eccentricity, the spheroid will be flattened about the minor axis [1]. Oblate spheroidal shells have many practical applications; two of these are liquid oxygen tanks used in several upper stages of space vehicles and the protective shell used as the housing of the early-warning scanner of Airborne Warning and Control System (AWACS) aircraft. Analytical solutions for such shells are inadequately investigated due to the complexity of the governing equations and the difficulty of obtaining their solutions [2]. Oblate spheroidal coordinates are the natural choice for the translation of any ellipsoid parallel to a principal axis [3]. There are many textbook examples giving applications of spheroidal coordinates. Some of the applications include the gravitational potential of an astronomical body, the solution to Maxwell's equations in electromagnetism, solid mechanics, and the study of various problems in quantum mechanics. A short history of the research work associated with the heat conduction with spheroidal coordinate system insights many novels and remarkable methods introduced by Green-Lam, Mathieu, Niven etc. The mathematical treatment of the problem of the conduction of heat for spheroids in terms of spheroidal wave functions was investigated dates back by Niven [4] which constitute a generalization of the corresponding solution for the sphere. Few highly cited literature on heat conduction in spheroid (prolate or oblate) making use of the spheroidal wave functions were considered by Flammer [5], Abramowitz and Stegun

* *E-mail: tarasadawarti@mail.com*

[6], Hodge [7], Meixner [8] and Li [9] in their books. Norminton and Blackwell [10] obtained the formal solutions for the transient heat flow from constant-temperature prolate and oblate spheroids as series in descending powers of the time, useful for large time calculations. Ozisik [11] gives the heat conduction equations in prolate and oblate spheroidal coordinate systems. Juncu [12] used numerical methods to investigate the transient heat transfer from an oblate/prolate spheroid to a steady stream of viscous, incompressible fluid. Alassar [13] obtained the analytical solutions of the problem of conduction heat transfer from oblate and prolate spheroids to an infinite medium. Very recently, Alassar [14] investigated two solutions of the problem, first by making use of the spheroidal wave functions and other by using an implicit finite difference scheme for an unsteady heat conduction from a spheroid (prolate or oblate). However, it was observed from the previous literature that almost all researchers have considered heat conduction without internal heat source subjected to radiation conditions. Things get further complicated when internal heat generation persists on the object under consideration and further becomes unpredictable when sectional heat supply is impacted by the body. Both analytical and numerical techniques have proved to be the best methodology to solve such problems. Nonetheless, numerical solutions are preferred and prevalent in practice, due to either non-availability or mathematical complexity of the corresponding exact solutions. Rather, limited utilisation of analytical solutions should mustn't diminish their merit over numerical ones; since exact solutions, if available, provide an insight into the governing physics of the problem, that is often missing in any numerical solution. In this regards Gupta [15] has introduced an integral transform applicable to spheroidal wave functions analogous to finite Fourier transform which applies to few boundary value problem relating to spheroids. Wankhede [16] generalized the transforms defined by Gupta for the prolate spheroidal geometry. Moreover, analysing closed-form solutions to obtain optimal design options for any particular application of interest is relatively simpler. Thus, a set of an integral transform and its inverse theorem for a heat conduction problem for multilayered composites in an oblate spheroidal coordinate system subjected to internal heat supply and radiation type boundary conditions are needed to obtain an exact solution. Again this integral transform defined is nothing but the generalization of the transforms defined in [15, 16] by establishing the Sturm-Liouville transform for the composite region consisting of k-layers by considering series expansion of a function in terms of eigenfunctions of Sturm-Liouville linear homogeneous boundary value problem for the composite region consisting of k-layers. To the best of authors knowledge, no research work has been taken for the thermoelastic analysis of oblate spheroids with internal heat source subjected to prescribed temperature on the curved surface. Owing to the lack of research in this field, the authors have been motivated to conduct this study. In this present paper, the realistic problem of spheroids subjected to initial temperature is studied. The theoretical calculation has been considered using the dimensional parameter, whereas, graphical calculations are carried out using the dimensionless parameter. The success of this research mainly lies on the new mathematical procedures which present a much more straightforward approach for optimization of the design in terms of material usage and performance in engineering problem, particularly in the determination of thermoelastic behaviour in spheroids engaged as pressure vessels, furnaces, etc.

2. Formulation of the Problem

We consider a composite oblate spheroidal shell occupying space $D : \{(\xi, \eta) \in R^2 \colon \xi_i < \xi < \xi_{i+1},\ -1 < \eta < 1\},\ 1 \leq i \leq k$. We assume that each rigid layer is homogeneous and isotropic, with thermal properties independent of temperature and that the layers are in imperfect thermal contact at the interfaces, which is characterised by the finite interfacial conductances $h_i > 0,\ i = 1, 2, ..(k-1)$. The internal heat sources are arbitrary but integrable functions of space and time. These are also called volume (bulk) source function, surface source function and interfacial source function respectively. Initially, the temperature distribution in each layer is given by an arbitrary but integrable function of space. These latter are also called

initial excitations or initial source functions. Under these prescribed source conditions and considerably general boundary and interfacial conditions, we wish to determine the transient temperature distribution in each layer of composite shell.

2.1. Temperature distribution

The differential equation governing transient temperature distribution $\theta_i(\xi,\eta,t)$ with internal heat source for a composite oblate spheroidal shell defined by [16] in the i^{th} layer as

$$\lambda_i\,\nabla^2\theta_i + Q_i(\xi,\eta,t) = (\rho C_v)_i\;\theta_{i,t}\,,\xi_i < \xi < \xi_{i+1},\;\; -1<\eta<1,\;\; i=1,2..k,\; t>0 \tag{1}$$

subjected to initial and boundary conditions

$$\begin{aligned}
\theta_i(\xi,\eta,0) &= \Theta_i(\xi,\eta)\\
h_0\theta_i(\xi,\eta,t) - \alpha_1\theta_i(\xi,\eta,t)_{,\xi}\,|_{\xi=\xi_1} &= f_1(\eta,t),\;\; h_0\geq 0,\\
h_k\theta_k(\xi,\eta,t) + \alpha_k\theta_k(\xi,\eta,t)_{,\xi}\,|_{\xi=\xi_{k+1}} &= f_2(\eta,t),\;\; h_k\geq 0,\\
\alpha_i\theta_i(\xi,\eta,t)_{,\xi}\,|_{\xi=\xi_{i+1}} &= \alpha_{i+1}\theta_{i+1}(\xi,\eta,t)_{,\xi}\,|_{\xi=\xi_{i+1}}\\
[\theta_{i+1}(\xi_{i+1},\eta,t) - \theta_i(\xi_{i+1},\eta,t)]/R_i|_{\xi=\xi_{i+1}} &+ \bar{Q}_i(\eta,t),\;\; i=1,2,...(k-1)
\end{aligned} \tag{2}$$

in which $Q_i(\xi,\eta,t)$ denotes prescribed arbitrary volume source per unit volume per unit time, $\Theta_i(\xi,\eta)$ is the initial surrounding temperature, λ_i for thermal conductivity and heat capacity per unit volume $(\rho C)_i$ with ρ_i for density and C_i as specific heat for the i^{th} layer, respectively. the prime (,) in equations denotes differentiation with respect to the variable specified in the subscript, the Laplacian operator in spheroidal coordinates is represented as

$$\nabla^2 = \frac{1}{c^2\,(\xi^2+\eta^2)}\left[\frac{\partial}{\partial\xi}(1+\xi^2)\frac{\partial}{\partial\xi} + \frac{\partial}{\partial\eta}(1-\eta^2)\frac{\partial}{\partial\eta}\right]$$

with $f_1(\eta,t)$ and $f_2(\eta,t)$ represents sectional heat supply, c is the interfocal distance, and $\bar{Q}_i(\eta,t)$ denotes distributed heat source for the i^{th} layer, respectively. The physical significance of the interface boundary conditions [i.e. equation (2)] is as follows: (i) the finite value of the layer coefficient $h_i>0,\;\; i=1,2,..(k-1)$ in the first two lines of equation (2) represents a discontinuity of temperature at the corresponding interface, and (ii) last line of equation (2) implies that the heat flux is continuous at the same interface or perfect thermal conduct there.

2.2. Thermal displacements and thermal stresses

The components of displacement given by [17] vector are represented by

$$\begin{aligned}
2Gu_\xi &= \;\; h\,\bar{\alpha}\,\tfrac{\partial\varphi_0}{\partial\xi} \;+ ch\bar{\alpha}\left\{\bar{\beta}^2\,\tfrac{\partial\varphi_4}{\partial\eta} - 4(1-\upsilon)\,\beta\,\varphi_4\right\},\\
2Gu_\eta &= -h\bar{\beta}\,\tfrac{\partial\varphi_0}{\partial\eta} \;+ ch\bar{\beta}\left\{\bar{\alpha}^2\,\tfrac{\partial\varphi_4}{\partial\eta} - 4(1-\upsilon)\,\alpha\,\varphi_4\right\}
\end{aligned} \tag{3}$$

in which the notations were taken as $\alpha=\sinh\xi$, $\bar{\alpha}=\cosh\xi$, $\beta=\cos\eta$, $\bar{\beta}=\sin\eta$ for mathematical simplicity, while G and υ are the shear modulus and Poisson's ratio, respectively, and $h=2/c^2(\alpha^2+\beta^2)$. The potential functions must satisfy

$$\nabla_1^2\varphi_0 = K\theta,\;\nabla_1^2\varphi_4 = 0\,\text{with}\varphi_0 = 0\;\text{at}t=0 \tag{4}$$

where K is the restraint coefficient, and

$$\nabla_1^2 = h^2\bar{\alpha}^2(\partial^2/\partial\xi^2) + 2h^2\alpha(\partial/\partial\xi) + h^2\bar{\beta}^2(\partial^2/\partial\eta^2) + 2h^2\beta(\partial/\partial\eta)$$

The corresponding stress components defined by [17] are given by

$$\begin{aligned}
\sigma_{\xi\xi} &= h^2 \left\{\bar{\alpha}^2 \frac{\partial^2\varphi_0}{\partial\xi^2} - c^2h^2\bar{\beta}^2\left(\xi\frac{\partial\varphi_0}{\partial\xi} - \eta\frac{\partial\varphi_0}{\partial\eta}\right)\right\} + ch^2\left\{\bar{\alpha}^2\bar{\beta}^2\ \frac{\partial^2\varphi_4}{\partial\xi\,\partial\eta}\right. \\
&\quad \left. -\ \bar{\alpha}^2\beta\left[c^2h^2\bar{\beta}^2 + 2(2-\upsilon)\right]\frac{\partial\varphi_4}{\partial\xi} - \alpha\,\bar{\beta}^2[c^2h^2\bar{\alpha}^2 - (1-2\upsilon)]\,\frac{\partial\varphi_4}{\partial\eta}\right\} \\
\sigma_{\eta\eta} &= h^2 \left\{\bar{\beta}^2 \frac{\partial^2\varphi_0}{\partial\eta^2} - c^2h^2\bar{\alpha}^2\left(\xi\frac{\partial\varphi_0}{\partial\xi} - \eta\frac{\partial\varphi_0}{\partial\eta}\right)\right\} - ch^2\left\{\bar{\alpha}^2\bar{\beta}^2\ \frac{\partial^2\varphi_4}{\partial\xi\,\partial\eta}\right. \\
&\quad \left. -\ \bar{\alpha}^2\beta\left[c^2h^2\bar{\beta}^2 + (1-2\upsilon)\right]\frac{\partial\varphi_4}{\partial\xi} - \alpha\,\bar{\beta}^2[c^2h^2\bar{\alpha}^2 - 2(2-\upsilon)]\,\frac{\partial\varphi_4}{\partial\eta}\right\} \\
\sigma_{\xi\eta} &= h^2\bar{\alpha}\,\bar{\beta}\left\{-\frac{\partial^2\varphi_0}{\partial\xi\,\partial\eta} + c^2h^2\left(\xi\frac{\partial\varphi_0}{\partial\eta} - \eta\frac{\partial\varphi_0}{\partial\xi}\right)\right\} - ch^2\bar{\alpha}\,\bar{\beta}\left\{\tfrac{1}{2}\left(\bar{\alpha}^2\frac{\partial^2\varphi_4}{\partial\xi^2} - \bar{\beta}^2\frac{\partial^2\varphi_4}{\partial\eta^2}\right)\right. \\
&\quad \left. -\ \alpha\left[c^2h^2\bar{\beta}^2 - 2(1-\upsilon)\right]\frac{\partial\varphi_4}{\partial\xi} + \beta\left[c^2h^2\bar{\alpha}^2 + 2(1-\upsilon)\right]\frac{\partial\varphi_4}{\partial\eta}\right\}
\end{aligned} \tag{5}$$

and for traction free surface stress functions

$$\sigma_{\xi\xi} = \sigma_{\xi\eta} = 0,\ \ \xi = \xi_1 \tag{6}$$

The equations (1) to (6) constitute the mathematical formulation of the problem under consideration.

3. Solution for the Problem

3.1. Solution for temperature distribution

In order to solve fundamental differential equation (2) using the theory of integral transformation, firstly introducing a new integral transform of order n and m over the variable ξ and η as

$$\bar{f}_i(q_n) = \beta_i \int_{\xi_i}^{\xi_{i+1}} \int_{-1}^{1} (\xi^2 + \eta^2)\, \Phi_{i,n,m}(\xi,\eta) f_i(\xi,\eta)\, d\xi\, d\eta \tag{7}$$

in which $\Phi_{i,n,m}(\xi,\eta)$ is the kernel and $\bar{f}_i(q_n)$ is Sturm-Liouville transform for the composite region of $f_i(\xi,\eta)$ and weight function $(\xi^2+\eta^2)$ (refer Appendix C). The inversion theorem is given by

$$f_i(\xi,\eta) = \sum_{n=1}^{\infty} A(n)\, \Phi_{i,n,m}(\xi,\eta) \sum_{i=1}^{k} \bar{f}_i(q_n) \tag{8}$$

Applying the above Sturm-Liouville transform defined in equation (7) on equation (1), and using the boundary conditions (2), we obtain

$$\sum_{i=1}^{\infty} \bar{\theta}_i(q_n,t)_{,t} + K_n^2\, \bar{\theta}_i(q_n,t) = G(q_n,t) \tag{9}$$

subjected to

$$\bar{\theta}_i(q_n,0) = \bar{\Theta}_i(q_n) \tag{10}$$

in which $K_n = 2q_n/c$ with q_n^2 as the eigenvalue of the problem, and

$$\begin{aligned}
G(q_n,t) &= \sum_{i=1}^{\infty} \int_{\xi_1}^{\xi_{i+1}} \int_{-1}^{1} \Phi_{i,n,0}(\xi,\eta)\, Q_i(\xi,\eta,t)\, d\xi\, d\eta + \int_{-1}^{1} \Phi_{i,n,0}(\xi_{i+1},\eta)\, (\xi_{i+1}^2 + \eta^2)\, f_2(\eta,t)\, d\eta \\
&\quad + \int_{-1}^{1} \Phi_{i,n,0}(\xi_k,\eta)\, (\xi_k^2 + \eta^2)\, f_1(\eta,t)\, d\eta + \int_{-1}^{1} \sum_{i=1}^{k-1} [\Phi_{i,n,0}(\xi_{i+1},\eta) - \Phi_{i+1,n,0}(\xi_{i+1},\eta)](\xi_k^2 + \eta^2)\, \bar{Q}_1(\eta,t)\, d\eta
\end{aligned}$$

Applying Laplace transform on Equation (9) with Equation (10) and taking its inverse, we obtain

$$\sum_{i=1}^{k} \bar{\theta}_i(q_n,t)_{,t} = \exp(-K_n^2 t) \sum_{i=1}^{k} \bar{\Theta}_i(q_n) + \int_0^t \exp[-K_n^2(t-\tau)]\, G(q_n,\tau)\, d\tau \tag{11}$$

Finally applying the inverse transform defined on (8), we obtain the temperature distribution as

$$\theta_i(\xi,\eta,t) = \sum_{n=1}^{\infty} A(n)\,\Phi_{i,n,0}(\xi,\eta) \sum_{i=1}^{k} \bar{\theta}_i(q_n,t),_t \tag{12}$$

A more explicit form of Equation (12) using Equation (11) can be expressed as

$$\begin{aligned}\theta_i(\xi,\eta,t) = \sum_{n=1}^{\infty} A(n)\,\Phi_{i,n,0}(\xi,\eta) \sum_{i=1}^{k} \exp(-K_n^2 t)\\ \times \left\langle \sum_{i=1}^{k} \int_{\xi_i}^{\xi_{i+1}} \int_{-1}^{1} (\rho C_v)_i\,(\xi^2+\eta^2)\,\Phi_{i,n,0}(\xi,\eta)\,\Theta_i(\xi,\eta)\,d\xi\,d\eta \right.\\ + \int_0^t \exp(-K_n^2\tau) \left\{ \sum_{i=1}^{k} \int_{\xi_i}^{\xi_{i+1}} \int_{-1}^{1} (\xi^2+\eta^2)\Phi_{i,n,0}(\xi,\eta)\,Q_i(\xi,\eta.t)\,d\xi\,d\eta \right.\\ + \int_{-1}^{1} \Phi_{i,n,0}(\xi_{k+1},\eta)(\xi_{i+1}^2+1) f_2(\eta,\tau)\,d\eta\\ + \int_{-1}^{1} \Phi_{i,n,0}(\xi_k,\eta)(\xi_{i+1}^2+1) f_1(\eta,\tau)\,d\eta\\ \left.\left. + \int_{-1}^{1} \sum_{i=1}^{i-1} [\Phi_{i,n,0}(\xi_{i+1},\eta) - \Phi_{i+1,n,0}(\xi_{i+1},\eta)]\,\bar{Q}_i(\eta.t)\,d\eta \right\} d\tau \right\rangle\end{aligned} \tag{13}$$

3.2. Solution for thermal stresses

Now, we assume potential functions which satisfy condition (4) as,

$$\begin{aligned}\varphi_0^{(i)} = K \sum_{n=1}^{\infty} \sum_{i=1}^{k} \left\langle \frac{\Phi_{i,n,0}(\xi,\eta)\exp(-K_n^2 t)}{\sin 2\eta\,(-1+q_n)}\ [B_n\,\cos 2\xi + \sin 2\eta] - \frac{1}{q_n}\Phi_{i,n,0}(\xi,\eta) \right\rangle\\ + \int_0^t \exp(-K_n^2\tau) \left\{ \sum_{i=1}^{k} \int_{\xi_i}^{\xi_{i+1}} \int_{-1}^{1} (\xi^2+\eta^2)\Phi_{i,n,0}(\xi,\eta)\,Q_i(\xi,\eta.t)\,d\xi\,d\eta \right.\\ + \int_{-1}^{1} \Phi_{i,n,0}(\xi_{k+1},\eta)(\xi_{i+1}^2+1) f_2(\eta,\tau)\,d\eta\\ + \int_{-1}^{1} \Phi_{i,n,0}(\xi_k,\eta)(\xi_{i+1}^2+1) f_1(\eta,\tau)\,d\eta\\ \left. + \int_{-1}^{1} \sum_{i=1}^{i-1} [\Phi_{i,n,0}(\xi_{i+1},\eta) - \Phi_{i+1,n,0}(\xi_{i+1},\eta)]\,\bar{Q}_i(\eta.t)\,d\eta \right\} d\tau\end{aligned} \tag{14}$$

in which the arbitrary constant B_n is to be determined by using the condition (4), one obtains

$$B_n = -\frac{1}{q_n}\frac{\sin 2\eta}{\cos 2\xi} \tag{15}$$

and

$$\begin{aligned}\varphi_4^{(i)} = \sum_{n=1}^{\infty} \sum_{i=1}^{k} \Phi_{i,n,0}(\xi,\eta)\exp(-K_n^2 t)[P_n\,\cos 2\xi + Q_n \cos 2\eta]\\ + \int_0^t \exp(-K_n^2\tau) \int_{\xi_i}^{\xi_{i+1}} \int_{-1}^{1} (\xi^2+\eta^2)\Phi_{i,n,0}(\xi,\eta)\,Q_i(\xi,\eta.t)\,d\xi\,d\eta\,d\tau\end{aligned} \tag{16}$$

in which P_n and Q_n are the arbitrary constants which can to be determined from the traction free surface stress condition (6).

$$P_n = -\bar{\beta}^2 \sum_{n=1}^{\infty} \sum_{i=1}^{k} \frac{X_n Z_n + Y_n[W_n - Z_n(R_n + X_n)]}{2Y_n\beta q_n \Phi_{i,n,0}(\xi,\eta)\bar{\alpha}^2 \sin 2\xi_1 (2(-2+\upsilon) + c^2h^2\bar{\beta}^2)(R_n + X_n)} \tag{17}$$

$$Q_n = \sum_{n=1}^{\infty} \sum_{i=1}^{k} \frac{X_n Z_n + Y_n W_n}{Y_n(2\,q_n\Phi_{i,n,0}(\xi,\eta)(\bar{\beta}^2\cos 2\eta\ + 2\beta(-1+\upsilon)\sin 2\eta) + (X_n\,S_n)} \tag{18}$$

where,

$$W_n = q_n c^2 h^2 \bar{\alpha}^2 \beta + 2\Phi_{i,n,0}(\xi,\eta)\cos 2\eta c h^2 K(-1+q_n)\xi_1,$$

$$
\begin{aligned}
X_n &= -\bar{\beta}^2(\alpha(-2+2\upsilon+c^2h^2\bar{\beta}^2)-\bar{\alpha}^2\cot 2\xi_1),\\
Y_n &= \beta\,\bar{\alpha}^2(2(-2+\upsilon)+c^2h^2\bar{\beta}^2),\\
Z_n &= c\,h^2(2\,K\,\Phi_{i,n,0}(\xi,\eta)(-1+q_n)\eta\,\cos 2\eta + c\,q_n\bar{\alpha}^2\alpha)\\
S_n &= 2\,q_n\,\Phi_{i,n,0}(\xi,\eta)\alpha\,(-1+2\upsilon)\sin 2\eta\\
R_n &= 2q_n\Phi_{i,n,0}(\xi,\eta)\,(\cos 2\eta\,\bar{\beta}^2+2\beta(-1+\upsilon)\,\sin 2\eta)/S_n
\end{aligned}
$$

Substituting the value of constant B_n from (15) in Equation (14), P_n and Q_n from Equation (17) and (18) into the Equation (16), one obtains the equation for potential functions.

3.3. Thermal displacements and thermal stresses

By substituting the above values of potential functions into the components of displacement vector Equation (3), one obtains

$$
\begin{aligned}
u_\xi^{(i)} = {}& \tfrac{1}{2G}c\,h\sum_{n=1}^{\infty}\sum_{i=1}^{k}\{-4\beta(1-\upsilon)\Phi_{i,n,0}(\xi,\eta)[\cos 2\eta(X_nZ_n+2ch^2K(-1+q_n)\\
&\times Y_n\xi_1\Phi_{i,n,0}(\xi,\eta)\cos 2\eta+c^2h^2q_n\beta\,Y_n\bar{\alpha}^2)/V_2-\bar{\beta}^2\cos 2\xi\ \csc 2\xi_1(X_n\,S_n/Y_n\\
&+2\,c\,h^2\ K(-1+q_n)\ \xi_1\Phi_{i,n,0}(\xi,\eta)\cos 2\eta+\beta\,\bar{\alpha}^2c^2h^2q_n-(X_n+R_n)Z_n)/V_1]\\
&+\tfrac{\bar{\beta}^2}{V_1\,V_2^2}\Phi_{i,n,0}(\xi,\eta)(-2\,V_1(X_n\,Z_n+4\,c\,h^2K(-1+q_n)\,Y_n\,\xi_1\Phi_{i,n,0}(\xi,\eta)\cos 2\eta\\
&+\beta\,\bar{\alpha}^2c^2h^2\,Y_n\,q_n)\,V_2\sin 2\eta\ -V_1\cos 2\eta\,(X_n\,Z_n+2\,c\,h^2K(-1+q_n)\,\xi_1\,Y_n\\
&\times\Phi_{i,n,0}(\xi,\eta)\cos 2\eta+\beta\,\bar{\alpha}^2c^2h^2\,Y_n\,q_n)\,V_{2,\eta}+\bar{\beta}^2\,V_2^2\cos 2\xi\csc 2\xi_1\\
&\times(4\,c\,h^2K(-1+q_n)\,\xi_1\,\Phi_{i,n,0}(\xi,\eta)\ \sin 2\eta+Z_n\,R_{n,\eta}+(X_n\,R_n)\,Z_{n,\eta})\}
\end{aligned}
\tag{19}
$$

$$
\begin{aligned}
u_\eta^{(i)} = {}& \tfrac{1}{2G}\,h\,\bar{\beta}\sum_{n=1}^{\infty}\sum_{i=1}^{k}\{-2K(-1+q_n)\,\Phi_{i,n,0}(\xi,\eta)\,\cos 2\eta/q_n+c\,[-4\,\alpha\,(1-\upsilon)\\
&\times\Phi_{i,n,0}(\xi,\eta)\,(\cos 2\eta\,(X_n\,Z_n+2\,c\,h^2K(-1+q_n)\,Y_n\,\xi_1\Phi_{i,n,0}(\xi,\eta)\cos 2\eta\\
&+\beta\,\bar{\alpha}^2c^2h^2Y_n\,q_n)/\,V_2-\bar{\beta}^2\cos 2\xi\ \csc 2\xi_1(X_n\,S_n/Y_n+2\,c\,h^2\,K\\
&\times(-1+q_n)\,\xi_1\,\Phi_{i,n,0}(\xi,\eta)\ \cos 2\eta+\beta\,\bar{\alpha}^2c^2h^2q_n-(X_n+R_n)Z_n)/V_1)\\
&-\tfrac{\bar{\alpha}^2}{V_1\,V_2^2}\Phi_{i,n,0}(\xi,\eta)(2\,V_1(X_n\,Z_n+4\,c\,h^2K(-1+q_n)\,\xi_1\,Y_n\,\Phi_{i,n,0}(\xi,\eta)\cos 2\eta\\
&+\beta\,\bar{\alpha}^2c^2h^2Y_n\,q_n)\,V_2\sin 2\eta+V_1\cos 2\eta\,(X_n\,Z_n+2\,c\,h^2K(-1+q_n)\,\xi_1\,Y_n\\
&\times\Phi_{i,n,0}(\xi,\eta)\cos 2\eta+\beta\ \bar{\alpha}^2c^2h^2Y_n\,q_n)\,V_{2,\eta}\ -\bar{\beta}^2\,V_2^2\cos 2\xi\ \csc 2\xi_1\\
&\times(4\,c\,h^2K(-1+q_n)\,\xi_1\,\Phi_{i,n,0}(\xi,\eta)\sin 2\eta+Z_n\ R_{n,\eta}+(X_n\ R_n)\,Z_{n,\eta})\,)]\,\}
\end{aligned}
\tag{20}
$$

in which

$$
\begin{aligned}
V_1 &= 2q_n(X_n+R_n(\eta))\beta\,\bar{\alpha}^2\Phi_{i,n,0}(\xi,\eta)(-4+2\upsilon+c^2h^2\,\bar{\beta}^2)\\
V_2 &= Y_n(X_n\,S_n+2q_n\Phi_{i,n,0}(\xi,\eta)\cos 2\eta\,\bar{\beta}^2+4q_n\beta(-1+\upsilon)\Phi_{i,n,0}(\xi,\eta)\sin 2\eta)
\end{aligned}
$$

The resulting equations of stresses can be obtained by substituting the Equation (14) and Equation (16) in Equation (5). The equations of stresses are rather lengthy. Consequently the same has been omitted here for the sake of brevity, but have been considered during graphical discussion using MATHEMATICA software.

4. Numerical Results, Discussion and Remarks

We introduce the following dimensionless values

$$
\left.
\begin{aligned}
&\bar{\xi}_i=\xi_i/b,\ \bar{a}=a/b,\ \bar{b}=b/b,\ e=c/b,\ \tau=\kappa\,t/b^2,\\
&\bar{\theta}=\theta/\theta_0,\ \bar{\sigma}_{mn}=\sigma_{mn}/E_i\,\alpha_i\,\theta_0,\ (i=1,2,3;\ m,\ n=\xi,\eta)
\end{aligned}
\right\}
\tag{21}
$$

For the sake of simplicity of numerical calculations, we consider a three-layered composite elliptic annulus plate. The numerical computations have been carried out for Aluminium, Tin and copper metal with zero initial temperature and for ($t > 0$) the temperature raised to finite value. The physical parameters are considered as $\bar{\xi}_1 = a = 0.1$ m, $\bar{\xi}_4 = b = 1$ m, $\bar{\xi}_2 = 0.4$ m, $\bar{\xi}_3$=0.7m, reference temperature θ_0 as 150^0C. The mechanical material properties are considered as specific heat capacity at constant pressure C_{v1}=0.900 J/g^{0}C, C_{v2}=0.21 J/g^{0}C, C_{v3}=0.385 J/g^{0}C, Modulus of Elasticity, E_1= 69 GPa, E_2 = 47 GPa and E_3 = 117 GPa; Shear modulus, G_1 = 26 GPa, G_2 = 15.6 GPa, G_3 = 48 GPa; Poisson ratio, $\upsilon_1 = 0.35$, $\upsilon_2 = 0.325$ andυ_3= 0.34;Thermal expansion coefficient, $\alpha_1 = 23.0\times10^{-6}/^0$C, $\alpha_2 = 24.8\times10^{-6}$ $/^0$C, $\alpha_3 = 16.5\times10^{-6}$ $/^0$C; Thermal conductivity λ_1 = 204.2 Wm^{-1} K^{-1}, λ_2 = 66 Wm^{-1} K^{-1} andλ_3= 386 Wm^{-1} K^{-1}; $f_1(t)$=0^{0}C, $f_2(t)$=20^{0}C. Substituting the dimensionless value of equation (21) in the equation of temperature distribution and in its stress components, we obtain the expressions for the temperature and stresses for our numerical discussion. In order to examine the influence of heating on the plate, we performed the numerical calculation for all variables, and numerical calculations are depicted in the following figures with the help of MATHEMATICA software. Plotted Fig. 1-Fig. 10 illustrate the numerical results of temperature distribution and the thermal stresses of the oblate spheroidal shell due to internal heat generation within the solid. Fig. 1 shows the temperature distribution along $\bar{\xi}$- direction for different time parameters. In this figure, temperature increases gradually towards the outer end of each layer due to the combined effect of sectional heat supply and internal heat energy.

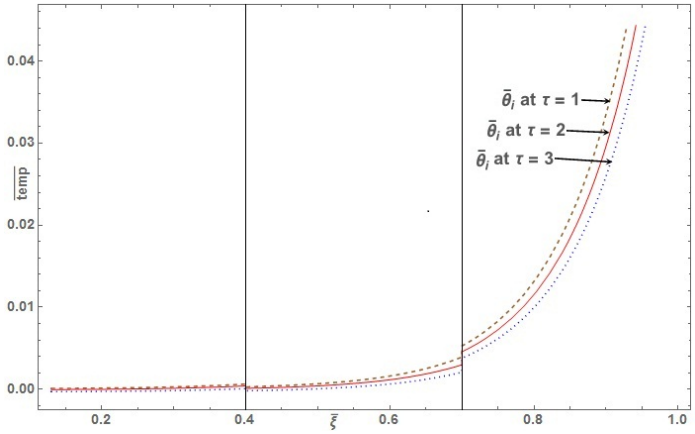

Figure 1. **Temperature distribution along $\bar{\xi}$ -direction for different τ.**

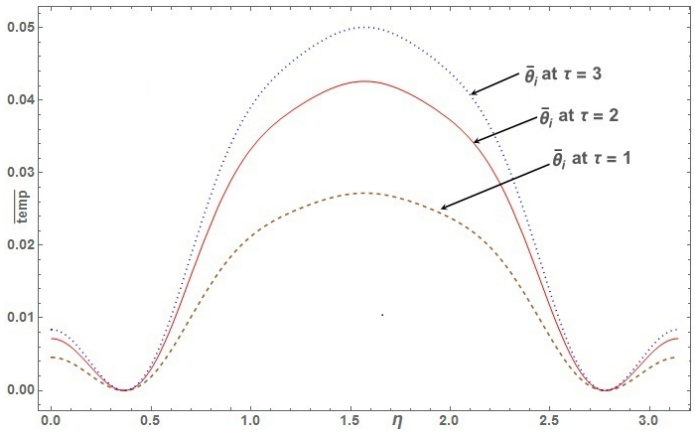

Figure 2. **Temperature distribution along η -direction for different time τ.**

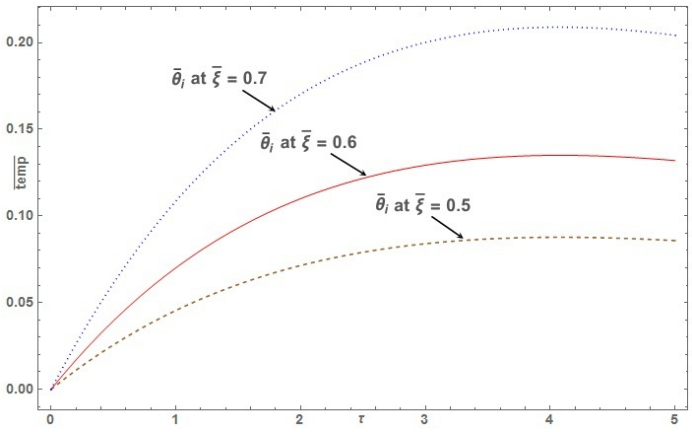

Figure 3. **Temperature distribution along time τ for different $\bar{\xi}$.**

As shown in Fig. 2, the temperature distribution along η-direction for different time parameters approaches to a minimum at both extreme ends i.e. at $\eta = 0$ and $\eta = \pi$ due to more compressive force, whereas due to a tensile force, the temperature is high at centre i.e. at $\eta = \pi/2$, which gives an overall bell-shaped curve for all three layers of different materials. Fig. 3 shows the time variation of the temperature distribution of the plate for various values of $\bar{\xi}$. Initially, the temperature profile approaches to zero, whereas increases gradually attaining the maximum value of temperature magnitude occurs as time increases due to the accumulation of energy from the available sectional heat supply. It was observed that further increase of time increases the temperature profile.

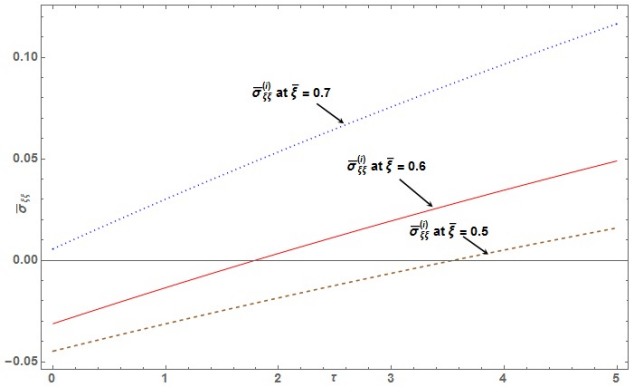

Figure 4. **Radial stress $\bar{\sigma}^{(i)}_{\xi\xi}$ along time τ for different $\bar{\xi}$.**

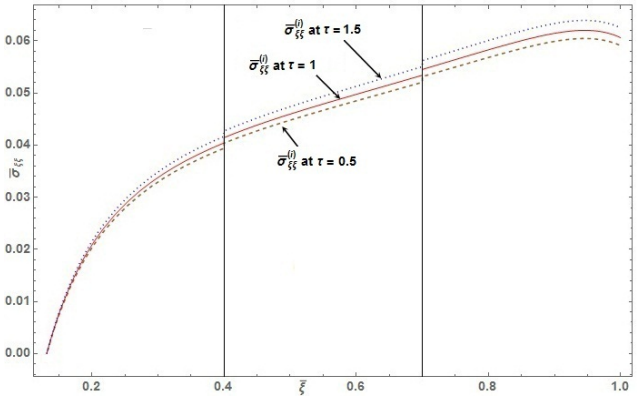

Figure 5. **Radial stress $\bar{\sigma}^{(i)}_{\xi\xi}$ along $\bar{\xi}$- direction for different time τ.**

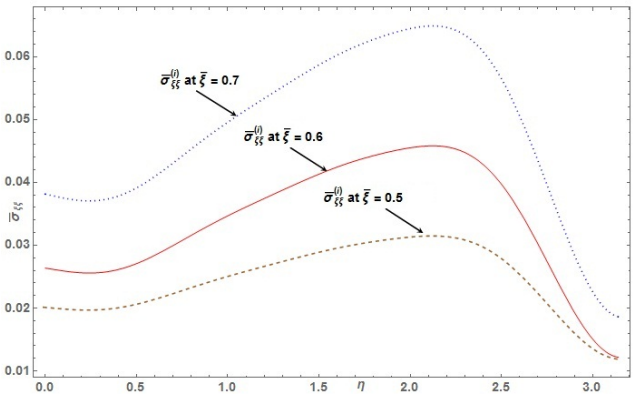

Figure 6. **Radial stress $\bar{\sigma}^{(i)}_{\xi\xi}$ along η for different $\bar{\xi}$.**

It is observed from the Fig. 4 that radial stress along time τ increases linearly from negative to positive values for different values of $\bar{\xi}$. Fig. 5 illustrates the axial stress along the $\bar{\xi}$- direction which is initially attained zero due to more compressive stress occurring at the inner edge which goes on increasing along the radius and attains a maximum at the outer edge. From Fig. 6, it is observed that the radial stress along the angular direction for different radius, the slight increase in radial stress due to the available internal heat source and heat accumulation due to sectional heat supply.

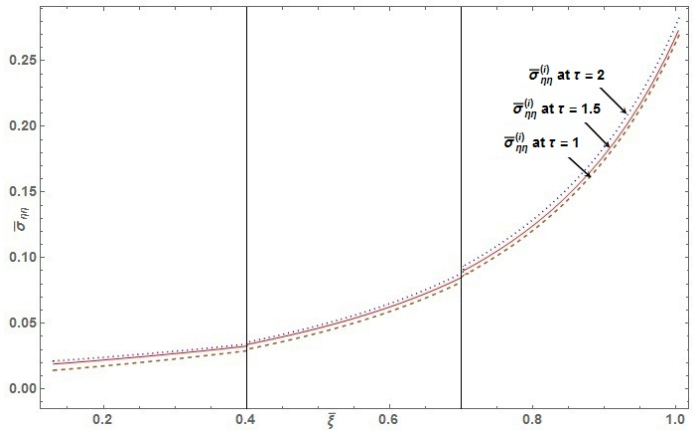

Figure 7. **Tangential stress $\bar{\sigma}^{(i)}_{\eta\eta}$ along $\bar{\xi}$- direction for different time τ.**

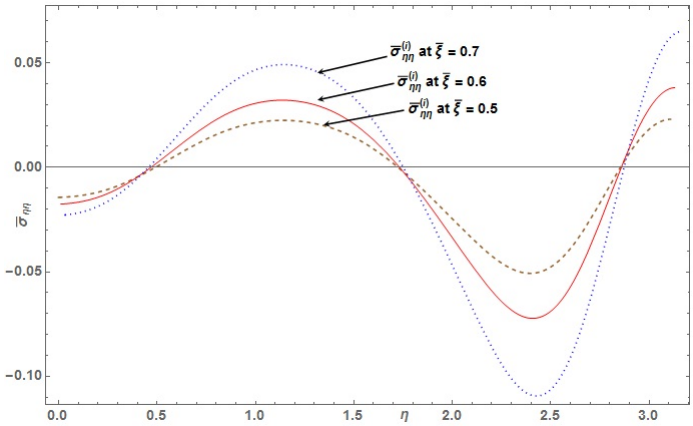

Figure 8. **Tangential stress $\bar{\sigma}^{(i)}_{\eta\eta}$ along η for different $\bar{\xi}$.**

Fig. 7 shows the tangential stress along the radial direction for different time, initially, minimum tangential stress occurs at the inner core whereas maximum stress occurs towards the outer end of each layer due to the internal heat energy and sectional heat supply. In Fig. 8, the tangential stress representing sinusoidal curve nature with a small crest and a large trough along the angular direction, thermal expansion occurs on the inner edge due to sectional heat supply and internal heat energy followed by the compressive stress occurring on the outer core of the ellipse. During analysis, it was observed

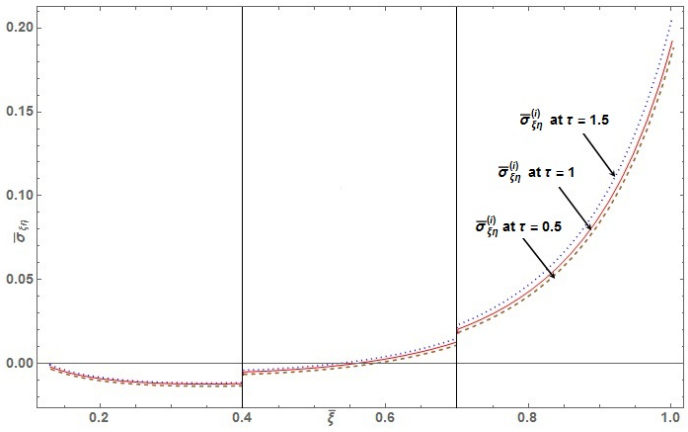

Figure 9. **Shear stress $\bar{\sigma}^{(i)}_{\xi\eta}$ along $\bar{\xi}$- direction for the different time τ.**

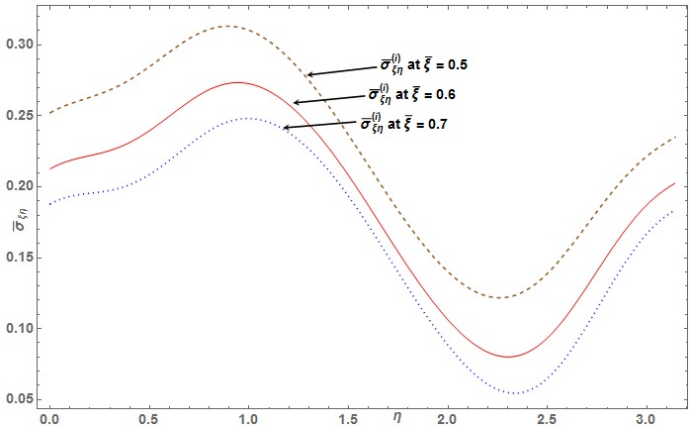

Figure 10. **Shear stress $\bar{\sigma}^{(i)}_{\xi\eta}$ along η for different $\bar{\xi}$.**

that the temperature distribution and stresses attain zero at $\bar{\xi} = \bar{\xi}_1$ satisfying the condition (6), which gradually increases along the radial direction and finally attains high at the outer edge. The above claim is illustrated in Fig. 1, Fig. 5, Fig. 7 and Fig. 9. In the foregoing investigation, as expected, there is an increment in the rate of heat propagation along a radius which leads to compressive force in the inner part and expands more on the outer surface whenever graph was plotted for temperature distributions, stress functions. Fig. 9 depicts shear stress along the angular direction; initially, stress goes on slightly increasing and suddenly decreases towards outer edge even with the growth of angles due to compressive force and again increases at the outer core. These changes could owe due to thermal expansion. Fig. 10 shows the changes of shear stress profile with different values of $\bar{\xi}$.

5. Conclusion

The proposed analytical solution of transient thermal stress problem in multilayer composites oblate spheroidal region was dealt in a spheroidal coordinates system with the presence of a source of internal heat. The integral transform defined in (7) is nothing but a generalization of the transforms defined in [15, 16] and the results can be deduced by specializing the coefficients and parameters involved therein. The analysis of non-stationary three-dimensional equation of heat conduction is investigated with the integral transformation method by establishing Sturm-Liouville integral transform considering series expansion function in terms of an eigenfunction of Sturm-Liouville boundary value problem. The following results were obtained during our research

1. The advantage of this method is its generality and its mathematical power to handle different types of mechanical and thermal boundary conditions.

2. The maximum tensile stress shifting from central core to outer part in the spheroidal region may be due to heat, stress, concentration or available internal heat sources under considered temperature field.

3. The maximum tensile stress occurring in the circular core on the major axis compared to spheroidal central part indicates the distribution of weak heating. It might be due to insufficient penetration of heat through the spheroidal inner surface.

4. Also by letting $d\xi/2 \to r$, $\eta \to \cos\theta$ as $\xi \to \infty$, where (r, θ) are spherical coordinates, we can obtain temperature distribution in the sphere.

5. Any particular case of interest can be deduced by assigning suitable values to the parameter and source functions involved in the solutions

References

[1] W. L. Gates, *Derivation of the equations of atmospheric motion in Oblate Spheroidal Coordinates*, Journal of the Atmospheric Sciences, 61(2005), 24782487.

[2] A. M. Al-Jumaily and F. M. Najim, *An approximation to the vibrations of oblate spheroidal shells*, Journal of Sound and Vibration, 204(1997), 561-574.

[3] R. F. Tuttle and S. K. Loyalka, *Gravitational collision efficiency of non-spherical aerosols II: motion of an oblate spheroid in a viscous fluid*, Nuclear Technology, 69(1985), 327336.

[4] C. Niven, *On the conduction of heat in ellipsoids of revolution*, Philosophical Transactions of the Royal Society of London, 171(1880), 117.

[5] C. Flammer, *Spheroidal Wave Functions*, Stanford University Press, Stanford, CA, (1957).

[6] M. Abramowitz and I. A. Stegun, *Handbook of Mathematical Functions*, 9th ed., Dover/New York (1970).

[7] D. B. Hodge, *Eigenvalues and eigenfunctions of spheroidal wave equation*, Journal of Mathematical Physics, 11(1970), 2308.

[8] J. Meixner, F.W. Schafke and G. Wolf, *Mathieu Functions and Spheroidal Functions and Their Mathematical Foundations*, Lecture Notes in Mathematics, vol. 837, Springer-Verlag, New York NY (1980).

[9] L. W. Li, X. K. Kang, L. W. Li, X. K. Kang and M. S. Leong, *Spheroidal wave functions in electromagnetic theory*, Wiley (2002).

[10] E. J. Norminton and J. H. Blackwell, *Transient heat flow from constant temperature spheroids and the thin circular disk*, The Quarterly Journal of Mechanics and Applied Mathematics, 17(1964), 6572.

[11] M. N. Ozisik, *Heat conduction*, Wiley, New York, (1993).

[12] G. Juncu, *Unsteady heat transfer from an oblate/prolate spheroid*, International Journal of Heat and Mass Transfer, 53(2010), 3483-3494.

[13] R. Alassar, M. Abushosha and M. El-Gebeily, *Transient heat conduction from spheroids*, Transactions of the Canadian Society for Mechanical Engineering, 38(2014), 373-389.

[14] R. Alassar, *Transient heat conduction from spheroids*, ASME Journal of Heat Transfer, 121(1999), 497-499.

[15] R. K. Gupta, *A finite transform involving spheroidal wave and its application*, Proc. Natn. Inst. Sci. India, 34A(1968), 289-300.

[16] P. C. Wankhede, *A study of some aspect of integral transforms with application to problems of physics and engineering*, PhD Dissertation University of Jabalpur, India (1972).

[17] E. Tsuchida and T. Uchiyama, *Stresses in an elastic circular cylinder with an oblate spheroidal cavity or internal penny-shaped crack under tension*, Bulletin of the JSME, 23(1980), 1-8.

[18] P. M. Morse and H. Feshbach, *Methods of Theoretical Physics*, McGraw Hill, New York, (1953).

[19] W. Magnus, F. Oberhettinger and R. P. Soni, *Formulas and Theorems for the Special Functions of Mathematical Physics*, Springer-Verlag, Berlin, Heidelberg, (1966).

Appendix A: THE REQUIRED TRANSFORMATION

1. The transformation and its essential property

Consider a system of equations for composite region consisting of k-layers

$$\alpha_i L\left[\psi_{i,n,m}(\xi,\eta)\right] = -\beta_i\, q_n^2(\xi^2+\eta^2)\,\psi_{i,n,m}(\xi,\eta),\ \ \xi_i \le \xi \le \xi_{i+1},\ -1 \le \eta \le 1,\ \ i = 1,\, 2, ...k \tag{A1}$$

subjected to the boundary conditions and interfacial boundary conditions

$$\left.\begin{aligned} -\alpha_1\psi_{i,n,m}(\xi,\eta)_{,\xi}\,|_{\xi=\xi_1} &= -h_0\psi_{i,n,m}(\xi,\eta)|_{\xi=\xi_1}\,, \qquad h_0 \ge 0,\\ \alpha_k\psi_{k,n,m}(\xi,\eta)_{,\xi}\,|_{\xi=\xi_{k+1}} &= -h_k\psi_{k,n,m}(\xi,\eta)|_{\xi=\xi_{k+1}}\,,\ \ h_k \ge 0,\\ \alpha_i\psi_{i,n,m}(\xi,\eta)_{,\xi}\,|_{\xi=\xi_{i+1}} &= \alpha_{i+1}\psi_{i+1,n,m}(\xi,\eta)_{,\xi}\,|_{\xi=\xi_{i+1}}\\ [\psi_{i+1,n,m}(\xi,\eta) - \psi_{i,m,n}(\xi,\eta)]/R_i|_{\xi=\xi_{i+1}}\,, &\quad i = 1,2,...(k-1) \end{aligned}\right\} \tag{A2}$$

in which

$$L = \frac{\partial}{\partial\xi}\left[(1+\xi^2)\frac{\partial}{\partial\xi}\right] + \frac{\partial}{\partial\eta}\left[(1-\eta^2)\frac{\partial}{\partial\eta}\right] + \frac{m\,(\xi^2+\eta^2)}{(1+\xi^2)(1-\eta^2)},$$

eigenfunction of the i^{th} layer is represented by $\psi_{i,n,m}(\xi,\eta)$, q_n^2 is the eigenvalue of the problem, $(\alpha_i\,,\beta_i)$ stands for the characteristics of the i^{th} layer, R_i denotes the characterises of the i^{th} interface, h_0 for the surface coefficients at $\xi = \xi_1$, and h_k for the surface coefficients at $\xi = \xi_{k+1}$, respectively. The general solution of equation (A1) is of the form

$$\Phi_{i,n,m}(\xi,\eta) = \left[A_{i,n}\,R^1_{nm}(\gamma_i c_n,\xi) + B_{i,n}R^2_{nm}(\gamma_i c_n,\xi)\right] S^1_{nm}(\gamma_i c_n,\eta),\ \gamma_i = (\alpha_i/\beta_i)^{1/2} \tag{A3}$$

satisfying the following boundary conditions, we get a system of $2k$ simultaneous equations so that arbitrary constants $A_{i,n}$ and $B_{i,n}$ can be obtained. Also from this $2k$ system of equations, we get the frequency equation by eliminating $A_{i,n}$ and $B_{i,n}$. After substituting the values of $A_{i,n}$ and $B_{i,n}$, we get the required solution of the Sturm-Liouville problem (A1) subjected to the boundary and interfacial conditions (A2).

2. Orthogonality of the eigenfunction $\psi_{i,n,m}$

If $\Phi_{i,n,m}$ and $\Phi_{i,s,m}$ be the solutions of Equation (A1), then we have

$$\alpha_i L\left[\Phi_{i,n,m}(\xi,\eta)\right] = -\beta_i\, q_n^2(\xi^2+\eta^2)\,\Phi_{i,n,m}(\xi,\eta) \tag{A4}$$

$$\alpha_i L\left[\Phi_{i,s,m}(\xi,\eta)\right] = -\beta_i\, q_s^2(\xi^2+\eta^2)\,\Phi_{i,s,m}(\xi,\eta) \tag{A5}$$

Multiplying Equation (A4) by $\Phi_{i,s,m}(\xi,\eta)$ and Equation (A5) by $\Phi_{i,n,m}(\xi,\eta)$, then subtract, and finally integrating with respect to η within -1 to 1 and with respect to ξ within ξ_i to ξ_{i+1}, we have

$$\begin{aligned}
&\sum_{i=1}^{k}\Bigg\langle \alpha_i \int_{\xi_i}^{\xi_{i+1}}\int_{-1}^{1}\{\Phi_{i,s,r}(\xi,\eta)\,[(1-\eta^2)\Phi_{i,n,m}(\xi,\eta),_\eta\,],_\eta \\
&-\Phi_{i,n,m}(\xi,\eta)[(1-\eta^2)\Phi_{i,s,m}(\xi,\eta),_\eta\,],_\eta\,\}d\xi\,d\eta \Bigg\rangle \\
&+\sum_{i=1}^{k}\Bigg\langle \alpha_i \int_{\xi_i}^{\xi_{i+1}}\int_{-1}^{1}\{\Phi_{i,s,r}(\xi,\eta)\,[(1+\xi^2)\Phi_{i,n,m}(\xi,\eta),_\xi\,],_\xi \\
&-\Phi_{i,n,m}(\xi,\eta)[(1+\xi^2)\Phi_{i,s,m}(\xi,\eta),_\xi\,],_\xi\,\}d\xi\,d\eta \Bigg\rangle \\
&=\sum_{i=1}^{k}\beta_i(q_s^2-q_n^2)\int_{\xi_i}^{\xi_{i+1}}\int_{-1}^{1}(\xi^2+\eta^2)\Phi_{i,n,m}(\xi,\eta)\Phi_{i,s,m}(\xi,\eta)\,d\xi\,d\eta
\end{aligned} \tag{A6}$$

and finally using the boundary and the interfacial conditions for the eigenfunctions $\Phi_{i,n,m}(\xi,\eta)$ and $\Phi_{i,s,m}(\xi,\eta)$, we find that the first and second group of terms on the left-hand side results to be zero. Hence from (A6) an orthogonality relation of the eigenfunctions $\Phi_{i,n,m}(\xi,\eta)$ can be expressed as

$$A(n)\sum_{i=1}^{k}\int_{\xi_i}^{\xi_{i+1}}\int_{-1}^{1}(\xi^2+\eta^2)\Phi_{i,n,m}(\xi,\eta)\Phi_{i,s,m}(\xi,\eta)d\xi\,d\eta \;=\delta_{ns}\;=\begin{cases}0, & \text{if } n\neq s\\ 1, & \text{if } n=s\end{cases} \tag{A7}$$

in which $\sqrt{A(n)}$ is the normalizing constant.

3. Property of the transform

Let us consider the effect of transform defined above

$$\begin{aligned}
&\sum_{i=1}^{k}\int_{\xi_i}^{\xi_{i+1}}\int_{-1}^{1}\beta_i\,(\xi^2+\eta^2)\,\Phi_{i,n,m}(\xi,\eta)L[f_i(\xi,\eta)]\,d\xi\,d\eta \\
&=\int_{-1}^{1}\{\Phi_{i,n,m}(\xi_{i+1},\eta)\,(\xi_{i+1}^2+1)\,[\alpha_i\,\psi_{i,n,m}(\xi,\eta),_\xi+h_i\,\psi_{i,n,m(\xi,\eta)}]_{\,\xi=\xi_{i+1}}\,d\eta\} \\
&+\int_{-1}^{1}\Bigg\langle\sum_{i=1}^{i-1}\Phi_{i,n,m}(\xi_{i+1},\eta)\,(\xi_{i+1}^2+1)\,\{\alpha_i\,f_i(\xi,\eta),_\xi-[f_{i+1}(\xi,\eta)-f_i(\xi,\eta)]/R_i\,\}_{\xi=\xi_{i+1}}\,d\eta \\
&-\Phi_{i+1,n,m}(\xi_{i+1},\eta)(\xi_{i+1}^2+1)\,\{\alpha_{i+1}\,f_{i+1}(\xi,\eta),_\xi-[f_{i+1}(\xi,\eta)-f_i(\xi,\eta)]/R_i\,\}_{\xi=\xi_{i+1}}\,\Big\rangle\,d\eta \\
&-\int_{-1}^{1}\{\psi_{1,n,m}(\xi_1,\eta)(\xi_{i+1}^2+1)[\alpha_1\,f_1(\xi,\eta),_\xi-h_0\,f_1(\xi,\eta)]_{\xi=\xi_1}\}d\eta\Bigg\rangle-q_n^2\sum_{i=1}^{k}\overline{f_i}(q_n)
\end{aligned} \tag{A8}$$

Hence (A8) is the fundamental property of the Sturm-Liouville transform for the composite region.

Appendix B: OBLATE SPHEROIDAL COORDINATES

Here for the spheroidal wave functions, the notations used are given in Flammer [5] textbook.

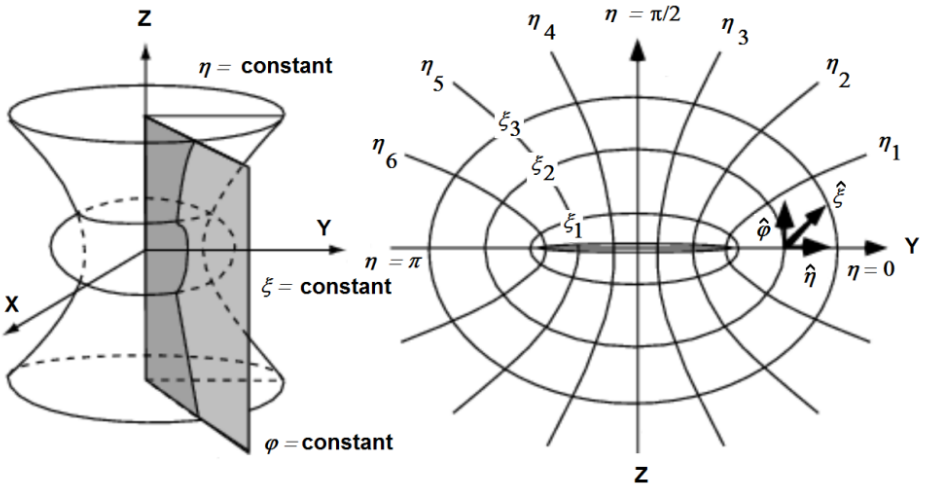

Figure 11. **The oblate spheroidal coordinate system**

For the present problems, it is convenient to use an oblate spheroidal coordinate system that can be established by revolving the two-dimensional elliptic coordinate system about the major axes of the ellipse [5] as shown in Fig. 11. The scale factors (metric coefficients) h_ξ, h_η and h_φ, for the oblate spheroidal coordinates system about rectangular coordinates (x, y, z) by the transformation can be taken as

$$x = c\,\sinh\xi\,\sin\eta\cos\varphi,\;\; y = c\,\sinh\xi\,\sin\eta\sin\varphi,\;\; z = c\,\cosh\xi\,\cos\eta \tag{B1}$$

alternatively, other equivalent transformation [18] from Equation (B1) as

$$\begin{aligned} x &= (c/2)\,(\xi^2-1)^{1/2}(1-\eta^2)^{1/2}\cos\varphi,\\ y &= (c/2)\,(\xi^2-1)^{1/2}(1-\eta^2)^{1/2}\sin\varphi,\\ z &= (c/2)\,\xi\,\eta \end{aligned} \tag{B2}$$

with either

$$-1 \le \eta \le 1,\;\; 0 \le \xi < \infty,\;\; 0 \le \varphi \le 2\pi,\;\; c > 0$$

or

$$0 \le \eta \le 1,\;\; -\infty \le \xi < \infty,\;\; 0 \le \varphi \le 2\pi,\;\; c > 0$$

moreover, the oblate spheroidal coordinate scale factors are given as

$$\left.\begin{aligned} h_\xi &= \left|\frac{\partial r}{\partial \xi}\right| = \tfrac{c}{2}\,\tfrac{(\xi^2+\eta^2)^{1/2}}{(1+\xi^2)^{1/2}},\\ h_\eta &= \left|\frac{\partial r}{\partial \eta}\right| = \tfrac{c}{2}\,\tfrac{(\xi^2+\eta^2)^{1/2}}{(1-\eta^2)^{1/2}},\\ h_\varphi &= \left|\frac{\partial r}{\partial \varphi}\right| = \tfrac{c}{2}(1+\xi^2)^{1/2}(1-\eta^2)^{1/2} \end{aligned}\right\} \tag{B3}$$

in which r is the Cartesian position vector of $r = xi + yj + zk$, $(\hat{\xi}, \hat{\eta}, \hat{\varphi})$ is the unit vectors defined as $[(\partial r/\partial\xi)/h_\xi, (\partial r/\partial\eta)/h_\eta, (\partial r/\partial\varphi)/h_\varphi)]$, c is the positive constant represents the semi-focal length, and here the metric coefficients are used to transform the governing equations from rectangular coordinates into the oblate spheroidal coordinate system [19].